ORIGINAL RESEARCH

Analysis of Characteristics Microvessel Density of Thyroid Malignant and Benign Nodules on Contrast-Enhanced Ultrasonography

Jingjing Liu, MD, Liping Liu, MD [*], Yanjing Zhang, MD, Yufang Zhao, MD, Yanhong Hao, MD, Tingting Li, MD, Xiaochun, Huang, MD

Department of Ultrasound, First Hospital of Shanxi Medical University, Taiyuan, China.
Received October 29, 2018; revision requested January 29, 2019; revision received November 12; accepted November 28.

Objective: To analyze the contrast-enhanced ultrasonography (CEUS) characteristics and microvessel density (MVD) of thyroid carcinomas vs. benign thyroid lesions, and to determine the value of CEUS in the clinical diagnosis of thyroid carcinoma.

Methods: Forty-five patients (34 women, 11 men; mean age, 45.95 ± 12.20 years) with 57 thyroid nodules underwent preoperative CEUS with SonoVue (injected as a bolus via an elbow vein). The CEUS data were analyzed using QLAB quantitative analysis software. The enhancement patterns and quantitative parameters of thyroid carcinoma were evaluated. Additionally, immunohistochemistry was performed to evaluate MVD.

Results: Most malignant nodules showed hypo-enhancement, and this enhancement pattern had 68.18% sensitivity and 92.31% specificity in diagnosing thyroid carcinomas. Most benign nodules showed ring enhancement, which had 46.15% sensitivity and 100% specificity in diagnosing benign nodules. Compared with the peripheral glandular tissue, thyroid carcinomas had significantly smaller peak intensities (PI) and wash-in slopes ($P < 0.05$). Malignant nodules had significantly lower MVD than benign nodules ($P < 0.05$). A positive correlation was between the PI and MVD ($P < 0.01$).

Conclusion: CEUS can improve the diagnosis of thyroid carcinomas, and is a useful complement to conventional ultrasonography.

Key words: Thyroid carcinoma; Contrast-enhanced ultrasound; Enhancement pattern; Microvessel density; Immunohistochemistry

Advanced Ultrasound in Diagnosis and Therapy 2018;03:167–172 DOI: 10.37015/AUDT.2018.180819

Thyroid nodules are the second most common endocrine disease [1,2]. The incidence of thyroid nodules has gradually increased in recent years, and almost 5%–15% of these nodules are malignant [3–8]. Conventional ultrasonography has emerged as the preferred imaging method for the diagnosis of thyroid diseases. However, the complexity of thyroid lesions and the overlapping ultrasonographic characteristics of benign and malignant nodules make a preoperative diagnosis difficult.

Compared with conventional ultrasonography, contrast-enhanced ultrasonography (CEUS) has been reported to improve the detection of malignant focal liver lesions [9,10]. It was a milestone for diagnostics in liver tumors. Recent studies have evaluated similar application of CEUS in characterizing thyroid gland tumors [11-15]. It is well known that the thyroid gland has an abundant microvasculature, and that the parenchyma of normal thyroid shows rapid and uniform enhancement after intravenous injection of contrast agents [16]. Moreover, the use of the second-generation ultrasound contrast agent SonoVue can

* *Corresponding author: Department of Ultrasound, First Hospital of Shanxi Medical University, Taiyuan, 030001, China.*
e-mail: liuliping1600@sina.com

improve the visualization of the microvasculature on CEUS by enhancing the backscatter of the blood flow to clearly depict tiny blood vessels within the lesion. This property is used to increase the blood flow difference between diseased and normal tissue, which has important implications for the differential diagnosis of benign and malignant lesions and can improve diagnostic accuracy.

Based on the Guidelines for clinical application of contrast-enhanced ultrasound in China, there are differences in the enhancement pattern of benign and malignant thyroid nodules. In this paper, we analyzed the CEUS characteristics and microvessel density (MVD) of thyroid carcinomas vs. benign thyroid lesions to determine the value of CEUS in the clinical diagnosis of thyroid carcinoma.

Patients and Methods

Patients

This study involved 45 patients with 57 pathologically confirmed thyroid nodules, and they were treated in our hospital between October 2013 and October 2014. All patients underwent conventional ultrasonography and CEUS before surgery. Informed consent was obtained from all patients or their families before examination.

CEUS image acquisition

In this study, we used the PHILIPS IU 22 color Doppler ultrasound machine equipped with a linear array transducer (5–12MHz), pulse inversion harmonic imaging technology and random analysis software. All thyroid nodules were evaluated, including location, size, shape, and blood-flow distribution, using both conventional ultrasonography and CEUS. In the long axis view, the entire nodule and the surrounding normal thyroid tissue were examined. If it was necessary to select a short-axis section, the contralateral normal thyroid tissue was used as a reference.

Before CEUS, we instructed the patients to calm themselves and not to swallow. We then switched to the contrast mode and placed the focus deeper than the nodule. Next, the patients were injected with a 2.4-mL bolus of suspending agent (SonoVue; Bracco, Italy) via a vein in the elbow, followed by 5 mL physiological saline, and press the key timing. Each nodule was scanned for at least 120 s. The enhancement of the nodules was observed, and dynamic images were recorded.

CEUS image analysis

The enhancement of the thyroid nodule relative to the surrounding tissue was categorized into hyper-, iso-, hypo-, and ring-enhancement patterns. In the last category, the periphery of the thyroid lesions exhibited enhancement, resembling a ring structure. Offline analysis was performed with QLAB. The region of interest was placed within the nodule over the thyroid parenchyma, taking care to avoid large blood vessels and calcifications. Spanning time intensity curve respectively, gamma curve were obtained by fitting the mathematical model of the gamma, provided by the curve of perfusion parameters with arrival time (AT), peak intensity (PI), mean transit time (MTT), wash-in slope (WIS), and time to peak (TTP).

Immunohistochemical analysis

We selected 30 large, paraffin-embedded thyroid tissue samples that had been preoperatively examined using CEUS for immunohistochemical staining. The wax block was frozen for 5 minutes and then sliced into 5μm-thick sections. The slices were baked for 3 h at 70°C and then deparaffinized with xylene, followed by 90% and 70% anhydrous alcohol (two times each). To eliminate endogenous peroxidase activity, we incubated the slices in 3% hydrogen peroxide solution for 15 min and then washed them with phosphate-buffered saline (PBS). The slices were placed in citrate buffer solution (pH, 6.0) and autoclaved for 2 min. The slices were washed again in PBS, incubated with mouse anti-CD34 monoclonal antibody (dilution, 1:100) at 37°C for 60 min, and re-washed in PBS. PV-9002 Polink-2 plus (two steps, reagents 1 and 2) was used as the secondary antibody, and the tissues were incubated with each reagent at 37°C for 15–20 min. The tissues were washed with PBS after incubation. Diaminobenzidine was added to the slices under a microscope to control the reaction time, and the slices were then rinsed with tap water. The slices were counterstained with hematoxylin, differentiated with 1% hydrochloric acid alcohol, and tap water blue. Finally, the slices were dehydrated in a gradient alcohol series, treated with xylene, and sealed with neutral balata.

MVD

MVD was calculated according to the double-blind method described by Weidner [17]. Under low magnification (×40), the area with highest number of microvessels was identified as a "hot spot," and the microvessels in this area were counted under high magnification (×200) [18]. Vessels with a luminal area greater than the diameter of eight red blood cells did not count as microvessels.

Statistics

Statistical analyses were performed using SPSS software (version 17.0). Count data were assessed using the chi square test. Quantitative CEUS characteristics of thyroid nodules and the surrounding glandular tissue were compared using the paired-samples

t-test. The MVDs of benign and malignant thyroid nodules were compared using the two independent-samples nonparametric test, the Mann–Whitney U test. Quantitative parameters and MVD were evaluated by the Spearman's Rank correlation analysis. $P < 0.05$ was considered to be a significant difference.

Results

General characteristics

Of the 45 study patients, 11 were men, and 34 were women. The mean age of the patients was 45.95 ± 12.20 years (range, 15–67 years). The maximum diameters of the lesions ranged from 3 to 48 mm. The 45 study patients had a total of 57 thyroid nodules, 44 nodules were malignant and 13 were benign. They were papillary carcinoma, 32; papillary microcarcinoma, 10; follicular variant of papillary microcarcinoma, 1; and medullary carcinoma, 1. Among the 13 benign nodules, 12 were nodular goiter and 1 with adenomatoid nodule.

CEUS

Of the 44 thyroid carcinomas in this study, 2 of them showed hyper-enhancement; 12 showed iso-enhancement; and 30 showed hypo-enhancement. Of the 13 benign nodules, 4 showed hyper-enhancement, 2 showed iso-enhancement, 1 showed hypo-enhancement, and 6 showed the ring enhancement. In total, 68.18% (30/44) of the thyroid carcinomas showed hypo-enhancement, and the sensitivity and specificity of this enhancement pattern in the diagnosis of thyroid carcinoma were 68.18% and 92.31%, respectively. Benign thyroid nodules mostly showed ring enhancement (46.15%, 6/13) or hyper-enhancement (30.77%, 4/13). The sensitivity and specificity of the ring-enhancement pattern in the diagnosis of benign thyroid nodules were 46.15% and 100%, respectively (Table 1).

Quantitative analysis of the CEUS images showed that compared with the surrounding glandular tissue, thyroid carcinomas had significantly lower PI and significantly smaller WIS ($P < 0.05$ for both) (Table 2).

Table 1 Enhancement pattern of 57 thyroid nodules

Group	hyper-enhancement	iso-enhancement	hypo-enhancement	ring-enhancement
Benign group	4	2	1	6
Malignant group	2	12	30	0
χ^2	4.807	0.258	14.801	18.061
P	0.028	0.611	< 0.001	< 0.001

Table 2 The comparison of quantitative CEUS parameters between thyroid malignant nodules and peripheral glands (Mean ± SD)

Group	*n*	RT	PI	MTT	WIS	TTP
Malignant nodules	44	9.43±6.72	6.68±5.23	11.96±6.59	0.64±0.51	24.28±14.46
Peripheral glands	44	8.58±5.57	10.53±6.72	13.41±8.19	1.20±0.72	22.61±7.12
t value		1.096	–4.602	–0.375	–6.385	1.094
P value		0.279	< 0.001	0.710	< 0.001	0.280

RT, arrival time; PI, peak intensity; MTT, mean transit time; TTP, time to peak; WIS, wash-in slope

Immunohistochemical analysis

The MVD of malignant thyroid nodules was 17.51 ± 3.38 per high-power field, while that of benign nodules was 27.67 ± 1.63 per high-power field. The MVD of malignant nodules was significantly lower than that of benign nodules ($P < 0.05$) (Table 3) (Fig. 1 and 2). A positive correlation existed between the PI and MVD (r_{CD34}=0.942, $P < 0.01$).

Table 3 The comparison of MVD counts between benign and malignant thyroid nodules (Mean ± SD)

Item	Malignant group	Benign group	*Z* value	*P* value
n	20	10		
AMC ± SD	17.51±3.38	27.67±1.63	–4.25	< 0.001

AMC, Average number of microvessel count; SD, Standard deviation

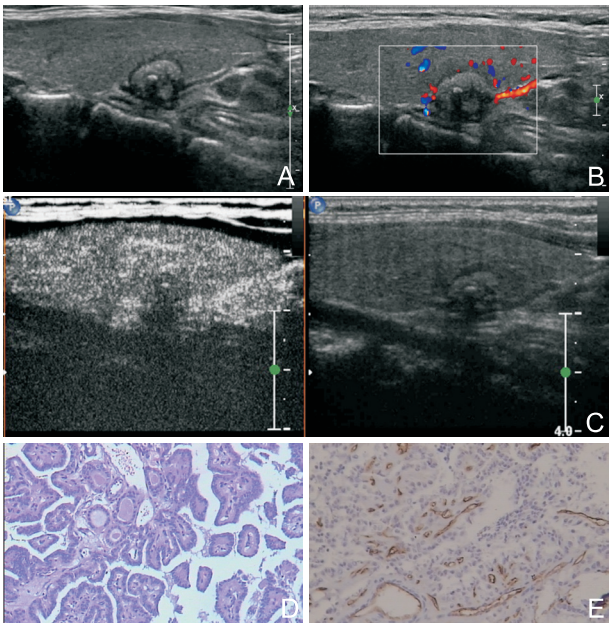

Figure 1 A 39-year-old female with a 1.13*0.91cm nodule in the left thyroid lobe. (A) Gray-scale US showed a hypoechoic solid nodule with calcification in the left lobe of the thyroid gland. (B) CDFI: There was no obvious blood flow in the nodule. (C) The nodule showed hypo-enhancement. (D) Surgical pathology showed a papillary thyroid carcinoma (HE, ×100). (E) Immunohistochemical staining of the thyroid nodule showed a lower microvessel density (CD34, ×100).

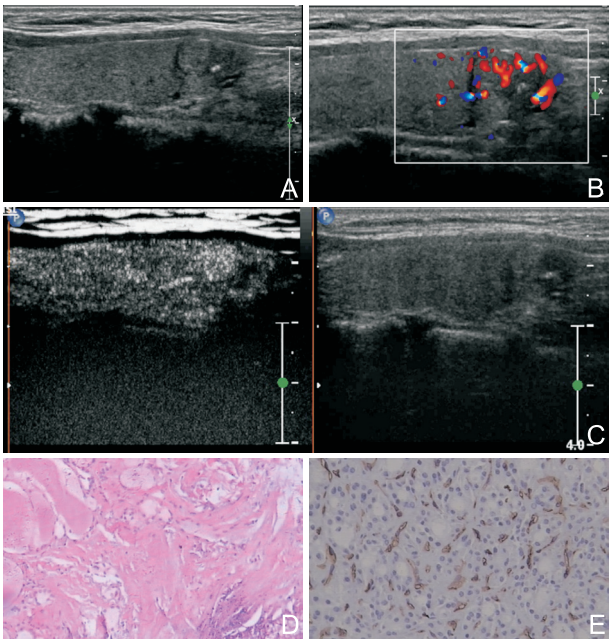

Figure 2 A 42-year-old female with a 1.03*0.91 cm nodule in the right thyroid lobe. (A) Gray-scale US showed a mixed echoic nodule with calcification in the right lobe of the thyroid gland. (B) CDFI: There were blood flow signals in the nodule. (C) The iso-echoic area of the nodule showed hyper-enhancement. (D) Surgical pathology showed a nodular goiter, part of follicular epithelial hyperplasia, interstitial fibrous tissue hyperplasia, hyaline change and calcification (HE, ×100). (E) Immunohistochemical staining of the thyroid nodule showed a higher microvessel density (CD34, ×100).

Discussions

As the most sensitive means of evaluating thyroid morphology, US can evaluate the size and characteristics of non-palpable nodules, and reveal lymph-node metastases. However, it is also well known that conventional US has a moderate accuracy for characterizing the nature of thyroid nodules depending on the tumor vasculature [19]. Color Doppler ultrasonography and Power Doppler ultrasonography detect mostly large blood vessels, and are not sensitive for detecting small intratumoral vessels. The use of the second-generation contrast agent SonoVue, a "blood pool-imaging agent," can compensate for the deficiencies of Doppler ultrasonography in this area. CEUS technology is a current research hot spot and is widely used in clinical practice. However, most research studies have investigated the use of CEUS in focal liver lesions; its application in thyroid nodules is a topic of ongoing research. The complex characteristics of thyroid nodules lead to differences in the enhancement patterns of benign and malignant thyroid nodules.

Zhang et al. [20] showed that ultrasound contrast perfusion differed between benign and malignant thyroid lesions. Most benign nodules showed ring enhancement, while inhomogeneous enhancement was mainly detected in malignant nodules in their study. Bartolotta et al. [21] considered that the size of thyroid nodules may affect their CEUS features; they found mainly diffuse contrast enhancement in nodules larger than 20mm, regardless of the histology, whereas nodules measuring less than 10mm lacked vascularization. They concluded that the enhancement pattern on CEUS was not specific to the diagnosis of thyroid carcinoma.

In our study, thyroid carcinomas mostly showed hypo-enhancement (30/44). This suggested that thyroid carcinomas had poor blood supply. These results were consistent with those of Moon et al and Deng J et al. [22-23]. The poor enhancement of thyroid carcinomas might be attributable to the following: (Ⅰ) during the development of thyroid carcinomas, cancer tissue invades the intratumoral blood vessels, leading to vascular necrosis; (Ⅱ) small, newly formed thyroid nodules may not yet possess abundant vasculature; (Ⅲ) tumor emboli may cause vascular stenosis or blockage [23]; and (Ⅳ) enhancement patterns depend on not only the quantity and shape of tumor vessels but also their patency, and not all intratumoral vessels are patent and functional. In this study, 12 malignant nodules showed iso-enhancement and 2-showed hyper-enhancement, which may be related to thyroid disease occurrence, development process. If the individual nodules are too

small, the enhancement and the boundary of the nodule are not clear, some nodules were due to its rich blood supply after enhancement compared with the surrounding without too much of the difference or show hyper-enhancement.

In this study, benign nodules were more likely to exhibit ring enhancement and hyper-enhancement. This may be explained by the fact that most benign nodules showed expansive growth, resulting in compression of the surrounding tissue; these nodules were encapsulated, and the blood vessels around the capsule give the appearance of ring enhancement on CEUS. Additionally, thyroid adenomas have abundant blood supply. In the present study, most benign thyroid nodule exhibited hyper-enhancement on CEUS. These results correspond with those reported by Moon et al. [22]. In our study, one benign thyroid nodule showed hypo-enhancement, which may be involved in calcification, fibrosis, hemorrhage and necrosis within the nodule.

Quantitative analysis of the CEUS images revealed that compared with the surrounding glandular tissue, thyroid carcinomas had significantly lower PI and WIS. WIS has also been shown to correlate with neo-arterisation. In addition, because of bits of neocapillaries, a small quantity of contrast agent would centralize in the tumor, thus resulting in a gentler WIS [24]. This result is consistent with the hypo-enhancement pattern of most thyroid carcinomas. RT, MTT and TTP are mainly affected by the blood flow rate. It indicates that there is no differences between the blood flow rate of thyroid carcinoma and the surrounding glands. The above parameters are more objective than macroscopic observation, and may therefore have clinical value in the diagnosis of thyroid carcinoma. Real-time dynamic CEUS observation of thyroid nodules can identify capsular invasion, which is difficult to detect on two-dimensional ultrasound, and is helpful for the diagnosis of thyroid carcinoma.

The MVD, which quantifies tumor angiogenesis, was evaluated using immunohistochemistry in our study. The analysis showed that malignant nodules had significantly lower MVD than benign nodules ($P < 0.05$), which further confirms that thyroid carcinomas have poor blood supply. This may be related to the occurrence of fibrosis and calcification in thyroid carcinomas. In addition, with improvement in ultrasonographic diagnosis, increasing number of lesions are detected early, when they have not yet developed rich vascular networks or formed arteriovenous fistulas. Moreover, a positive correlation existed between the PI and MVD. While contrast-enhanced ultrasound PI partly reflects MVD, it indirectly reflects the blood perfusion of the lesions. In conclusion, hypo-enhancement is an important CEUS pattern characteristic of malignant thyroid nodules.

Our study has several limitations. First, only some pathological types of thyroid nodules were studied. Second, the sample size of this study was small, and the proportions of benign and malignant nodules differed greatly; a larger sample size is required to definitively determine the CEUS characteristics of thyroid nodules. Third, only large lesions were subjected to immunohistochemistry, and the accuracy of our conclusions needs to be confirmed in smaller lesions.

Conclusion

In summary, the CEUS characteristics of thyroid nodules can facilitate the diagnosis of thyroid carcinoma, and potentially play a more important role in the noninvasive diagnostic approach, which has clinical significance.

Conflicts of interest

The authors have no conflict of interest to declare.

Acknowledgements

This research was supported by Scientific Research Projects for Returned Overseas Scholar of Shanxi Province (No. 2014-073) and Ministry of Human and Social Affairs Program for the selection of Science and Technology activities for Returned Overseas Scholar (No. 2016-366).

References

[1] Golden SH, Robinson KA, Saldanha I, Anton B, Ladenson PW. Prevalence and incidence of endocrine and metabolic disorders in the United States: a comprehensive review. *J Clin Endocrinol Metab* 2009; 94:1853–78.

[2] Roti E, degli Uberti EC, Bondanelli M, Braverman LE. Thyroid papillary microcarcinoma: a descriptive and meta analysis study. *Eur J Endocrinol* 2008; 159:659–73.

[3] Guth S, Theune U, Aberle J, Galach A, Bamberger CM. Very high prevalence of thyroid nodules detected by high frequency (13 MHz) ultrasound examination. *Eur J Clin Invest* 2009; 39: 699–706.

[4] Wiest PW, Hartshorne MF, Inskip PD, Crooks LA, Vela BS, Telepak RJ, et al. Thyroid palpation versus high−resolution thyroid ultrasonography in the detection of nodules. *J Ultrasound Med* 1998; 17: 487–96.

[5] Tomimori E, Pedrinola F, Cavaliere H, Knobel M, Medeiros−Neto G. Prevalence of incidental thyroid disease in a relatively low iodine intake area. *Thyroid* 1995;5: 273–6.

[6] Brander A, Viikinkoski P, Nickels J, Kivisaari L. Thyroid gland: US screening in a random adult population. *Radiology* 1991; 181: 683–7.

[7] Tunbridge WM, Evered DC, Hall R, Appleton D, Brewis M, Clark F, et al. The spectrum of thyroid disease in a community: the Whickham Survey. *Clin Endocrinol* (*Oxf*) 1977; 7: 481–93.

[8] Fish SA, Langer JE, Mandel SJ. Sonographic imaging of thyroid nodules and cervical lymph nodes. *Endocrinol Metab Clin N Am* 2008; 37: 401–17.

[9] Burns PN, Wilson SR, Simpson DH. Pulse inversion imaging of liver

blood flow: improved method for characterizing focal masses with microbubble contrast. *Invest Radiol* 2000; 35: 58−71.

[10] Burns PN, Wilson SR. Focal liver masses: enhancement patterns on contrast−enhanced images: concordance of US scans with CT scans and MR images. *Radiology* 2007; 242: 162−74.

[11] Minami Y, Kudo M: Ultrasound fusion imaging of hepatocellular carcinoma: A review of current evidence. *Dig Dis* 2014; 32: 690−5.

[12] Yu D, Han Y, Chen T: Contrast−enhanced ultrasound for differentiation of benign and malignant thyroid lesions: Meta. analysis. *Otolaryngol Head Neck Surg* 2014;151: 909−15.

[13] Jiang J, Huang L, Zhang H, Ma W, Shang X, Zhou Q, et al: Contrast-enhanced sonography of thyroid nodules. *J Clin Ultrasound* 2015; 43: 153−6.

[14] Nemec U, Nemec SF, Novotny C, Weber M, Czerny C, Krestan CR: Quantitative evaluation of contrast−enhanced ultrasound after intravenous administration of a microbubble contrast agent for differentiation of benign and malignant thyroid nodules: Assessment of diagnostic accuracy. *Eur Radiol* 2012; 22: 1357−65.

[15] Agha A, Jung EM, Janke M, Hornung M, Georgieva M, Schlitt HJ, et al, Preoperative diagnosis of thyroid adenomas using high resolution contrast−enhanced ultrasound (CEUS). *Clin Hemorheol Microcirc* 2013; 55: 403−9.

[16] Massimo G, Claudia C, Stefano G, Barbara M, Enzo S, Eleonora M, et al, The use of semi−quantitative ultrasound elastosonography in combination with conventional ultrasonography and contrast−enhanced ultrasonography in the assessment of malignancy risk of thyroid nodules with indeterminate cytology. *Thyroid Res* 2014; 7: 9.

[17] Weidner N. Current pathologic methods for measuring intratumor−al microvessel density within breast carcinoma and other solidtumors. *Breast Cancer Res Trest* 1995; 36: 169−80.

[18] Sener E, Sipal S, Gündoğdu C. Comparison of Microvessel Density with Prognostic Factors in Invasive Ductal Carcinomas of the Breast. *Turkish Journal of Pathology* 2016; 32: 164−70.

[19] Moon WJ, Baek JH, Jung SL, Kim DW, Kim EK, Kim JY, et al. Ultrasonography and the ultrasound−based management of thyroid nodules: consensus statement and recommendations. *Korean J Radiol* 2011; 12: 1−14.

[20] Zhang B, Jiang YX, Liu JB, Yang M, Dai Q, Zhu QL, et al. Utility of contrast−enhanced ultrasound for evaluation of thyroid nodules. *Thyroid* 2010; 20: 51−7.

[21] Bartolotta TV, Midiri M, Galia M, Runza G, Attard M, Savoia G, et al. Qualitative and quantitative evaluation of solitary thyroid nodules with contrast enhanced ultrasound: initial results. *Eur Radiol* 2006; 16: 2234−41.

[22] Moon HJ, Kwak JY, Kim MJ, Son EJ, Kim EK. Can vascularity at power Doppler US help predict thyroid malignancy? *Radiology* 2010; 255: 260–9.

[23] Deng J, Zhou P, Tian SM, Zhang L, Li JL, Qian Y. Comparison of Diagnostic Efficacy of Contrast−Enhanced Ultrasound, Acoustic Radiation Force Impulse Imaging, and Their Combined Use in Differentiating Focal Solid Thyroid Nodules. *Plos One* 2014; 9: e90674.

[24] Strouthos C, Lampaskis M, Sboros, V, McNeilly A. & Averkiou M. Indicatordilution models for the quantification of microvascular blood flow with bolus administration of ultrasound contrast agents. *IEEE Trans Ultrason Ferroelectr Freq Control* 2010; 57: 1296–310.